Investigation of the foil structure and corrosion mechanisms of modern Zwischgold using advanced analysis techniques

Author(s):
Wu, Qing; Soppa, Karolina; Scherrer, Nadim; Watts, Benjamin; Yokosawa, Tadahiro; Bernard, Laetitia; Araki, Tohru; Döbeli, Max; Meyer, Markus; Spiecker, Erdmann; Fink, Rainer H.

Publication date:
2018-05-01

Permanent link:
https://doi.org/10.3929/ethz-b-000261066

Originally published in:
Journal of cultural heritage 31, https://doi.org/10.1016/j.culher.2017.12.005

Journal of Cultural Heritage 31 (2018) 122–132

Available online at ScienceDirect www.sciencedirect.com

Elsevier Masson France EM|consulte www.em-consulte.com/en

Original article

Investigation of the foil structure and corrosion mechanisms of modern Zwischgold using advanced analysis techniques

Qing Wu[a,1,*], Karolina Soppa[a], Nadim Scherrer[a], Benjamin Watts[b], Tadahiro Yokosawa[c], Laetitia Bernard[d], Tohru Araki[e], Max Döbeli[f], Markus Meyer[c], Erdmann Spiecker[c], Rainer H. Fink[c]

[a] Bern University of Applied Sciences (BUAS) – Bern University of the Arts (BUA), Fellerstrasse 11, 3027 Bern, Switzerland
[b] Paul Scherrer Institute (PSI), 5232 Villigen PSI, Switzerland
[c] Friedrich-Alexander University Erlangen-Nürnberg (FAU), Schlossplatz 4, 91054 Erlangen, Germany
[d] Swiss National Laboratories of Material Science and Technology (Empa), Ueberlandstrasse 129, 8600 Dübendorf, Switzerland
[e] Diamond Light Source, Diamond House, Harwell Science & Innovation Campus, Didcot, Oxfordshire, United Kingdom
[f] Swiss Federal Institute of Technology in Zurich (ETHZ), Hönggerberg, 8093 Zurich, Switzerland

ARTICLE INFO

Article history:
Received 14 August 2017
Accepted 12 December 2017
Available online 3 January 2018

Keywords:
Zwischgold
Interdiffusion
Gold
Silver
Corrosion
Conservation

ABSTRACT

Zwischgold is a two-sided metal foil made by adhering a gold leaf over a silver leaf to present a gold surface while using less gold than gold foils. Corroded Zwischgold surfaces appear dark, accompanied by gloss loss and possible mechanical stability issues. Zwischgold applied artefacts are commonly found in museums and churches across Europe and they currently face an uncertain future as conservators have little knowledge to base conservation treatments on. We present a comprehensive material analysis of Zwischgold models through advanced characterization techniques including focused ion beam coupled with scanning electron microscopy (FIB-SEM), transmission electron microscopy (TEM), scanning transmission X-ray microscopy (STXM), time-of-flight secondary ion mass spectrometry (TOF-SIMS) and Rutherford backscattering spectrometry (RBS). Complementary information on the foil thickness, sharpness of the gold-silver interface, gold purity, and the formation as well as distribution of corrosion products on Zwischgold models have been obtained, representing a starting point for understanding the morphology and the long-term chemistry of Zwischgold artefacts.

1. Introduction

Gold surfaces have been highly valued in sculpture since ancient times. However, gold has also been a very expensive material to obtain [1–3], driving artisans to develop techniques to either simulate or economize the production of gold surfaces. In medieval times, a two-layered metal foil of gold backed by another metal (usually silver) became popular, largely because it allowed the gold layer to be made thinner and thus becoming cheaper than regular gold leaf at that time by at least half [3], while still presenting an actual gold surface [1,4,5]. This Zwischgold (German) [5–7], also called Twistgold [8], zwischt golt [9], gedeild guld [8], Zwischengolde [1], or part-gold (English) [1], is described in historical literature as using a "cold welding" technique [5,6] to adhere the layers together using only mechanical pressure.[2] Although Zwischgold was first mentioned by Theophilus in the 11th century for metalwork and metallic threads [11], the application of Zwischgold to works of art started from the beginning of the 13th century [1,12] and became popular in German sculptures in the 14th century [1,13]. As an economic alternative to pure gold foils [1,2,5,12,14–16], it was commonly applied in the non-prominent

* Corresponding author.
E-mail addresses: qingaling@gmail.com (Q. Wu), karolina.soppa@hkb.bfh.ch (K. Soppa), nadim.scherrer@hkb.bfh.ch (N. Scherrer), benjamin.watts@psi.ch (B. Watts), tadahiro.yokosawa@fau.de (T. Yokosawa), laetitia.bernard@empa.ch (L. Bernard), tohru.araki@diamond.ac.uk (T. Araki), doebeli@phys.ethz.ch (M. Döbeli), markus.meyer@fau.de (M. Meyer), erdmann.spiecker@fau.de (E. Spiecker), rainer.fink@fau.de (R.H. Fink).
[1] Permanent address of the corresponding author: Rütenentrasse 27, 5322 Koblenz, Switzerland.

[2] Cold welding or contact welding is a kind of solid-state welding process in which joining takes place without fusion/heating (i.e. at ambient temperature) at the interface of the two parts to be welded [10]. In the case of the production of Zwischgold in the Middle Ages, many historical literature have recorded that two metal thin plates (e.g., Au & Ag) were hammered together to make an ultra-thin metal foil that contained two metal layers.

https://doi.org/10.1016/j.culher.2017.12.005

areas of the sculpture or altarpiece such as the troughs of gown folds or the rear side of the figures [1,17,18], as well as under coloured glazing [9,12,15,18,19].

The historical and modern literature repeatedly records that the disadvantage of applying Zwischgold is that its surface tends to darken quickly in air, due to the vulnerability of the silver base to corrosion on exposure to atmosphere. Therefore, the application of Zwischgold was often prohibited or strictly controlled by the guild regulations of medieval cities [1,8]. In the regions where Zwischgold use was allowed, the application of a protective varnish layer (e.g., mixture of drying oil and resin) over the Zwischgold surface during the manufacture of the artefacts was usually suggested or required [15,20–22]. However, after hundreds of years, patches of darkened surface on artefacts applied with Zwischgold can be observed in many museums, churches, private collections or other historical sites (Fig. 1), which could be attributed to the

Fig. 1. The wooden sculpture "Hl. Bischof" in the Basel Historical Museum, 15c. Zwischgold is present in the darkened areas inside of the red frame.

aging mechanisms (or possible removal by cleaning processes) of the varnish layer so that it no longer provides sufficient protection to the Zwischgold.

Besides the widely accepted economic reason, other reasons for the application of Zwischgold such as aesthetics, iconography and symbolism are recorded in historical literature and discussed by many historians [12,15,19]. For example, Zwischgold was quite often applied (with oil gilding techniques) to the hair of the figures [15,18,23], due to its paler or colder colour tone compared to pure gold [12,22–24]. Other typical examples of the purposeful application of Zwischgold are the Ortenberger Altar [12] in the Hessian State Museum (Darmstadt) and the Leiggerner Altar [25] in the Swiss National Museum (Zurich), where gold and Zwischgold were extensively applied in different prominent areas, presenting a significant aesthetic contrast. Scientific analyses of Zwischgold artefacts can aid in understanding the art history and art technologies found in the object.

2. Research aims

Nowadays most conservators hold a cautious and restrained attitude regarding the conservation of Zwischgold, due to a lack of knowledge of the material. Our analyses should help conservators to understand Zwischgold and thus provide a scientific foundation for conservation treatments in future. Therefore, we aim to link the material science aspects of gold and silver to the art technology of Zwischgold and to demonstrate useful techniques for the investigation of Zwischgold. In this work, we present a starting point for the study of Zwischgold through the use of advanced analytical techniques to characterize the foil structure and aging mechanisms of Zwischgold models. Discussion of the measurements will be restricted to those illustrative of scientific insights, while the full set of data is provided in the Supplementary data, along with an index (Table S1).

3. Theories

Zwischgold has so far received little attention in scientific studies and only a few publications report on the materials analysis of Zwischgold [12,26–32]. In most of these publications, Zwischgold is only marginally described and not enough scientific detail is provided to understand its corroded states. To our knowledge, so far the only image showing a clear structure and corroded states of Zwischgold is presented in *Louvre Crucifix by Giotto* by Eveno et al. [26]. The Doerner Institute (Munich), Royal Institute for Cultural Heritage (IRPA-KIK, Brussels) and the Lower Saxony State Museum (Hannover) are currently collaborating to study the *Goldene Tafel from Lüneburg*, where metal foils have been investigated via X-ray fluorescence analysis (XRF) and scanning electron microscopy coupled with energy dispersive X-ray analysis (SEM-EDX). However, Zwischgold is not easy to differentiate from gold-silver alloy through such techniques [33]. On the other hand, there exists a great deal of scientific literature on gold and silver (as discussed in the following sections), as well as their alloys, that can be drawn on to inform and focus our studies of Zwischgold. Since gold is well known to be inert to oxidizing species, silver is clearly the main participant in the corrosion chemistry of Zwischgold, while theories on the diffusion of gold and silver help to explain why the expectedly pure gold surface of Zwischgold tends to accumulate dark coloured silver corrosion products.

3.1. Gold and silver interdiffusion

Gold and silver are both noble metals with very similar atomic radii and crystal structure [10]. Further, they are completely miscible in alloys [34]. On the other hand, silver is more reactive, has a lower atomic mass (and thus lower material density also) and has a slightly lower surface energy of 1140 mJm^{-2} [35] compared to gold (1250 mJm^{-2} [36]) that causes gold-silver alloys to tend to have silver-enriched surfaces.

At high temperatures, silver and gold atoms are able to diffuse (i.e. move by jumping between lattice positions) in the alloy crystals, but this becomes frozen at temperatures close to ambient. However, Hwang et al. [34] observed silver diffuse through a polycrystalline gold film and accumulate of the surface at temperatures as low as 47 °C, where lattice diffusion is not energetically possible. This diffusion occurred at the boundaries of the gold grains, where the disorder of the mismatching adjacent gold lattices provides opportunities for lower-energy atomic movements. For thin films of gold, as is found in Zwischgold, the grains of gold will tend to be significantly wider than the film thickness and so have columnar shape that means the grain boundaries provide relatively direct paths across the film. The room temperature migration of silver to the top surface is therefore surprisingly efficient, with a significant surface concentration of silver being detectable after a period of hours or days [37]. Since the diffusion rate of silver is higher than that of gold, a grain-boundary Kirkendall effect is observed, in which the mass gained or lost by the unequal diffusion in the grain boundaries is compensated for by a mass flow in a direction perpendicular to the grain-boundary plane [34]. This effect causes the gold grain boundaries to open wider, allowing easier transit for further silver, while silver atoms in the silver layer will tend to move towards the gain boundaries, continuously resupplying the grain-boundary regions such that there is a constant source of silver atoms for the grain-boundary diffusion. The grain-boundary Kirkendall effect further causes vacancies to accumulate inside of the silver layer, lowering its mass density.

Hwang et al. [34] also show that there should be a saturation depth for the silver accumulation layer corresponding to at least several atomic layers and silver atoms are distributed uniformly over the surface in the lateral direction and concentrated homogeneously in the top two monolayers before saturation is reached. This thin silver layer on the top Zwischgold surface could explain the relatively colder colour tone of Zwischgold compared to pure gold. However, this equilibrium thickness of silver varies, depending on the surface energy difference, the driving force of surface corrosion and other factors [37].

3.2. Silver corrosion

Upon exposure to air, the top atomic layer of silver will quickly oxidize, lowering the surface energy to 500 mJm^{-2} [35]. However, this monolayer oxide is quite stable when dry and further chemical reactions do not occur at ambient temperatures in the absence of water. Water adsorbed on the silver surface provides a medium for the dissolution of oxidizing gaseous compounds such as hydrogen sulphide (H_2S) and carbonyl sulphide (COS) in the atmosphere and the subsequent dissolution of silver and precipitation of corrosion products [38]. Silver sulphide, Ag_2S, is the most prominent corrosion product of silver, which has been well discussed in the literature [38–41]. The thickness of the adsorbed water layer increases with humidity, thus enabling an increase in the rate of corrosion.

The gold and silver diffusion theories as well as the silver corrosion mechanisms outlined above indicate that it is likely to observe significant changes in the foil structure after the initial layering of gold over silver. Therefore, we have applied nanoscale analysis techniques to investigate the foil structure and chemical states of Zwischgold models in order to assess how these theories correspond to the practical situation. We observe silver corrosion products on the top surface of the Zwischgold, that the gold layer

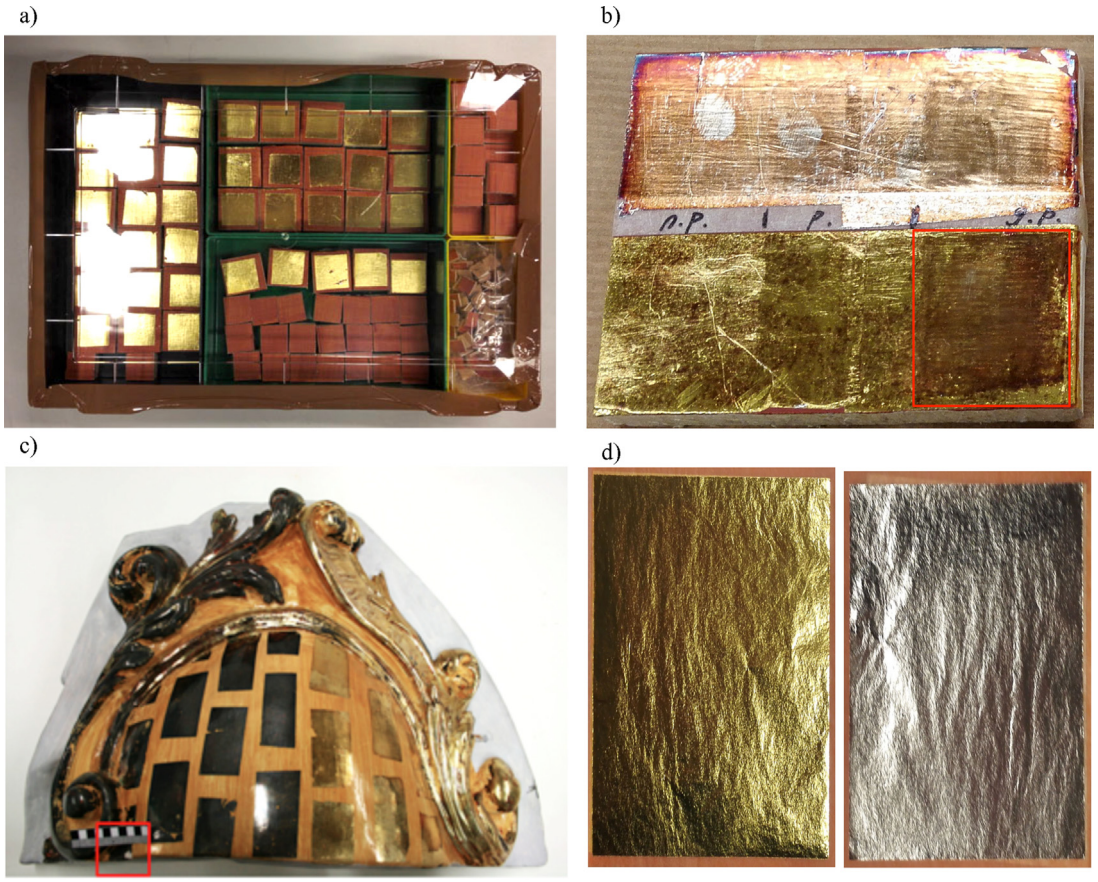

Fig. 2. Zwischgold models/object used in the investigation: a: non-aged Zwischgold models, stored in nitrogen-filled box; b: 3-month naturally aged Zwischgold model, in which silver foils (in the upper part) were also applied besides Zwischgold for the purpose of comparison; c: 35-year old Zwischgold object exhibited at BUAS-CR; d: freestanding Zwischgold foil: gold side (left) and silver side (right). Samples were taken from the areas inside of the red frames.

is not as pure as the manufacturer states it was initially, and the formation of large voids in place of the original silver layer – all in agreement with the above theories of interdiffusion and silver corrosion mechanisms.

4. Materials and methods

4.1. Sample preparation

Unvarnished Zwischgold models were produced in the Conservation-Restoration Division at Bern University of Applied Sciences (BUAS-CR), based on the bole gilding recipes recorded in *Liber Illuministarum* [42]. The applied Zwischgold foils were purchased from *Noris Blattgold* (Schwabach, Germany). The stratigraphic structure of non-aged Zwischgold models, as well as the procedures and materials of model production are presented in Supplementary data (S1). The surfaces of some models were burnished with an agate tool. Non-aged samples (burnished and non-burnished) were stored in a nitrogen-filled box, preventing oxidation (Fig. 2a). Some burnished models were exposed to an indoor environment ($23 \pm 2\,^{\circ}C$ and $50 \pm 2\%$ RH) for natural aging over a period of 3 months (Fig. 2b). Besides the recently produced Zwischgold models, a 35-year old Zwischgold object[3] (Fig. 2c) was also sampled, by taking advantage of a demonstration artefact at BUAS-CR. Freestanding Zwischgold foils were used as samples for certain experiments (Fig. 2d).

Sample cross-sections cut by ultra-microtomy[4] and focused ion beam (FIB) were provided for SEM experiments. Cross-sectional thin slices were prepared either by ultra-microtomy for transmission electron microscopy (TEM; 50 nm thick), scanning transmission X-ray microscopy (STXM; 350–400 nm), or by FIB for scanning transmission electron microscopy (STEM; 50 nm). The time-of-flight secondary ion mass spectrometry (TOF-SIMS) and Rutherford backscattering spectrometry (RBS) experiments did not require special sample preparation as they probe the layers directly. However, these Zwischgold samples were trimmed to an appropriate size and the wooden substrate thinned in order to minimize outgassing in the experiments vacuum chamber.

4.2. Experiments

As a practical analysis tool for obtaining the morphological and compositional information of the sample, SEM-EDX was initially used for investigating the foil structure and elemental associations of the Zwischgold samples at BUAS ("Zeiss EVO SEM"). In order to avoid artefacts caused by conventional sample preparation methods (embedding and mechanic sanding/cutting), same samples were also prepared and investigated through FIB-SEM "FEI Helios Nanolab 660" in the Centre for Nanoanalysis and Electron Microscopy (CENEM) at the Friedrich-Alexander University Erlangen-Nürnberg (FAU, Erlangen, Germany). The accelerating voltage and beam current in the FIB-SEM experiments was set to

[3] The 35-year old Zwischgold object was produced in 1982 by Ulrich Schiessl, a German art historian and restorer (1948–2011) [43].

[4] Knife "Diatome Ultra 45", clearance angle 6°, knife angle 45°.

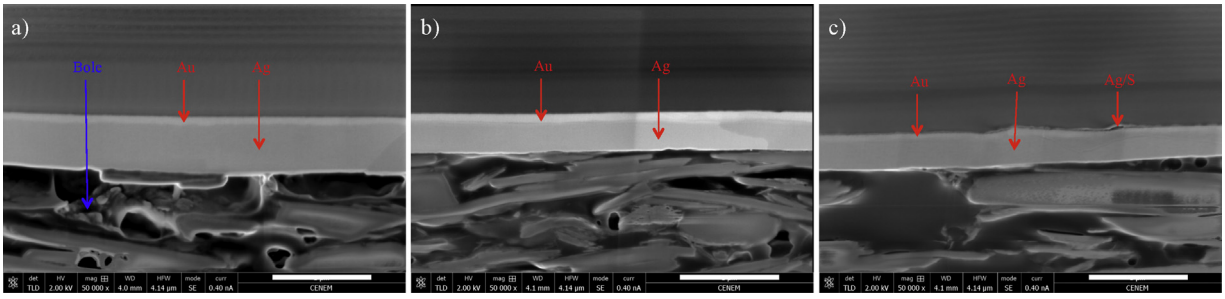

Fig. 3. Secondary electron (SE) micrographs through "FEI Helios Nanolab 660" for three different Zwischgold model cross-sections (Mag 50,000): a: "na_nb", b: "na_b"; c: "a3m_b". Scale bar: 1 μm.

2 kV and 0.40 nA respectively for obtaining high-resolution electron images. The accelerating voltage was then raised to 5 kV for element identification and mapping through EDX, with quantitative mapping performed by spectral peak-fitting via the instrument's integrated "AZtec" software.

In order to get more detailed information about the 35-year old sample, the double aberration-corrected high-resolution TEM "Titan Themis3 300" was used at CENEM. During the experiments, the STEM mode coupled with EDX was operated for the imaging and the elemental identification (quantitative mapping performed by spectral peak integration via the instrument's integrated software). Conventional TEM experiments were also implemented through the "Zeiss EM900" instrument at FAU.

Synchrotron-based STXM experiments were performed at beamline I08 in the Diamond Light Source, (Didcot, United Kingdom) to measure nanoscale, quantitative element maps of Zwischgold cross-sections. The X-ray beam is focused with a Fresnel zone plate (25 nm outermost zone width for a spot size of about 30 nm). Transmission mode images were recorded at photon energies spanning 2200–3400 eV in order to image the samples at the Au $M_{4,5}$-, S K- and Ag L_3-edges. Quantitative STXM data analysis and element mapping (S8 in Supplementary data) was performed using the MANTiS analysis software [44].

To acquire detailed information on the Au/Ag interface and the direct molecular assessment of the corrosion products, TOF-SIMS experiments were implemented in the Swiss National Laboratories of Material Science and Technology (Empa, Dübendorf, Switzerland). Depth profiling (depth resolution ~2 nm) was performed using a 25 keV Bi_1^+ analysis beam in high mass resolution mode and combined with a 1 keV Cs^+ sputter beam. Negative secondary molecular ions were detected from mass 1 to 800 Da on randomly selected areas of $100 \times 100\ \mu m^2$ (with concentric sputter area of $500 \times 500\ \mu m^2$).

In addition, RBS, a non-destructive quantitative analysis technique, was also applied for obtaining the compositional depth information of non-aged Zwischgold samples. Measurements were performed at the Swiss Federal Institute of Technology (ETH, Zurich, Switzerland) laboratory for Ion Beam Physics, using a 2 MeV ^4He beam and a silicon PIN diode detector at 168°.

5. Results and discussion

5.1. Structure and foil thickness of modern Zwischgold foils

FIB-SEM micrographs of the non-aged and non-burnished ("na_nb"), non-aged and burnished ("na_b"), and 3-month aged and burnished ("a3m_b") Zwischgold model cross-sections are presented in Fig. 3. The contrast in these micrographs depends on the density of the material, so gold appears the brightest and the silver slightly darker, while the bole materials (consisting of silicon, aluminium, oxygen and carbon) are even darker. The layered structure of Zwischgold is clearly observed, with a relatively thinner gold layer above a thicker silver layer. The metal layers appear smooth and are cleanly cut through by FIB; the heterogeneous bole is below the foil. Note that Sample "a3m_b" (Fig. 3c) shows an uneven top surface compared to "na_nb" (Fig. 3a) and "na_b" (Fig. 3b), which is attributed to an extra thin layer above the Au layer. EDX measurements identified S and Ag as the main compositional elements in this top layer (S4.2 in Supplementary data), indicating the presence of silver sulphide. This will be discussed in detail in Section 5.4.

Fig. 4 shows the RBS measurements for non-aged Zwischgold samples ("na_nb" and "na_b"). While modeling is required to extract detailed information, some general meaning can be read from RBS spectra: the peak positions provide information on the elements present (heavier atoms appear further right), their depth below the surface (the peak is swept further to the left at greater depths) and the purity of the layer (by comparing the observed peak height to reference spectra). The gold and silver layers of the Zwischgold samples are clearly visible as separate regimes in Fig. 4 and the relative layer thicknesses correspond to the width of these peaks. The RBS data for the "na_nb" sample fits well to a model involving a 100 nm layer of 92% Au and 8% Ag (by atom ratio) over a 445 nm thick 100% Ag layer, while the "na_b" data fits well to a similar model with a 108 nm layer of 92% Au on a 490 nm 100% Ag layer. The RBS spectra will be further discussed in Sections 5.2 and 5.3.

Thicknesses of the gold and the silver layers measured with FIB-SEM and RBS, as well as the overall thickness of the Zwischgold foil measured with TEM (S6 in Supplementary data) and STXM (Fig. 6) are summarised in Table 1. There are variations between some of these measurements that do not consistently correlate with model finishing treatments (such as burnishing) or the sample preparation techniques used. Therefore we expect that the observed thickness differences represent variations in the manufacture of the Zwischgold foils. We conclude that the overall thickness of modern Zwischgold foil varies in the range of 500–700 nm and the gold layer is equal to or less than 110 nm.

5.2. The gold and silver interface

RBS indicates that the interface between the gold and silver layers of Zwischgold is some combination of rough and/or diffuse for non-aged samples. The fitting models for the "na_nb" and "na_b" data involve an area-integrated composition gradient between the two layers (combining the effects of interface roughness and intermixing) having a sigmoid profile with a thickness of 90 nm and 104 nm, respectively. TOF-SIMS depth profiling offers a more detailed view into the chemical speciation at and around the interface by analysing fragments of material removed while sputtering a crater into the sample. Fig. 5 presents depth profiles performed on the non-aged ("na_b") and aged ("a3m_b") samples. Both profiles clearly show the gold and silver layers of the Zwischgold foil via

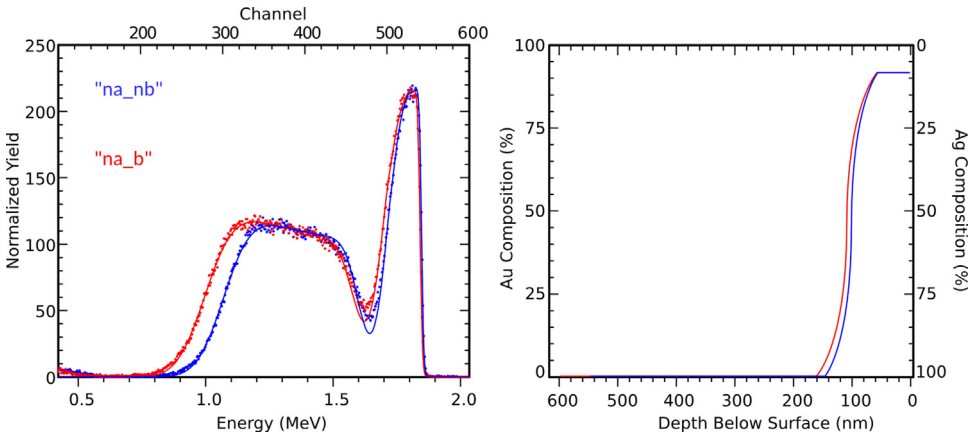

Fig. 4. 2 MeV He RBS spectra for Zwischgold samples: "na_nb" (in blue) and "na_b" (in red). Flat background has been subtracted.

Table 1
Respective thickness of the Au and the Ag layer inside the Zwischgold foil (or overall foil thickness) for different samples, measured by different analytical methods.

	Non-aged, non-burnished (nm)	Non-aged, burnished (nm)	3-month aged, burnished (nm)
FIB-SEM (Au/Ag)	93 ± 11/603 ± 23	94 ± 9/383 ± 11	58 ± 16/373 ± 27
RBS (Au/Ag)	100/445	108/490	–
TEM (overall)	560–600[a]	~590	~600
STXM (overall)	~650	–	~380

[a] Measured from a freestanding foil.

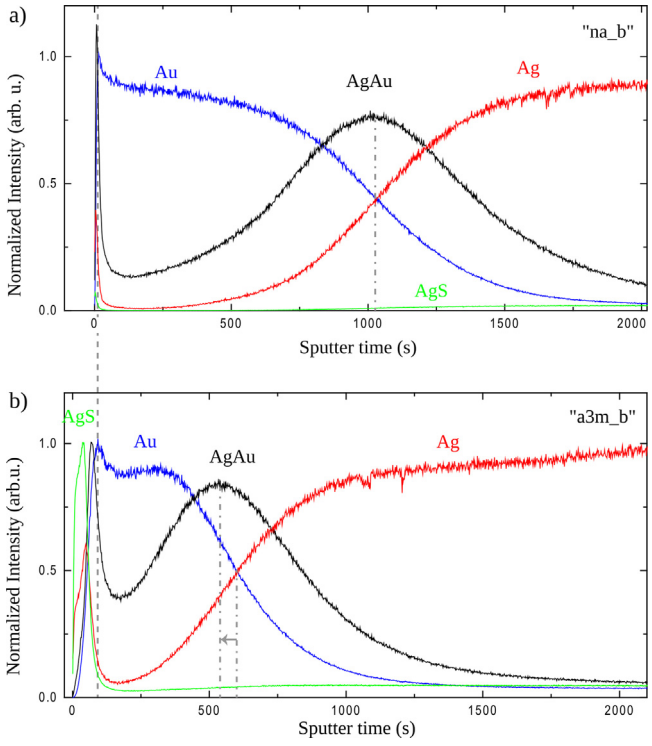

Fig. 5. TOF-SIMS depth profiles of characteristic secondary ions of Zwischgold samples: a: "na_b"; b: "a3m_b": Au (Au_2^- + Au_4^-, blue curve), Ag (Ag^- + $Ag_3{}^{109}Ag_2^-$, red curve), AgAu ($AgAu^-$ + $AgAu_2^-$, black curve) and AgS (AgS^- + $^{109}AgS^-$, green curve). Note that the profiles were normalized to 1 to increase the visibility. The x-axis (sputter time) is representing the depth of the analysis into the Zwischgold and was shifted to align the Au top surface in both measurements (dashed grey line). The dashed-dotted grey line represents the Au/Ag interface centre and the AgAu intermixing layer centre (they coincide in "a" but not in "b").

the dominance of the "Au" signal (blue curve) in the shallower, low sputter time region and the "Ag" (red curve) signal in the deeper, high sputter time region. The gold layer in "a3m_b" is observed to be about 60% as thick as that in "na_b", in agreement with the thickness measurements by FIB-SEM in Table 1. The "AgAu" signal (black curve) shows a broad peak in the region of the gold-silver interface, similar in width to the respective gold layers.[5] This signal corresponds to the detection of ions consisting of gold and silver atoms bonded together, indicating atomic-level mixing of these elements and proving that the gold-silver interface is diffuse. Further, the diffuseness of the interface shown by TOF-SIMS indicates that the RBS composition gradient should be dominated by this diffuse nature and there must be little roughness of the interface (i.e. little variation in gold layer thickness within each sample). While the "AgAu" maximum position aligns well with the crossing of the "Au" and "Ag" signals in Sample "na_b" (Fig. 5a), the "AgAu" maximum in "a3m_b" (Fig. 5b) is shifted into the gold layer compared to the crossing of the "Au" and "Ag" signals (indicated with arrow). This observation strongly supports the hypothesis that the intermixing is predominantly governed by Ag diffusion into Au, as discussed in Section 3.1.

Examining the surface region of "a3m_b" (near zero sputter time in Fig. 5b) clearly shows a series of three distinct peaks of the "AgS" (green curve), "Ag" and "AgAu" signal before the gold layer begins at ~100 s (indicated by a dashed line). The first "AgS" peak indicates a silver sulphide layer with a significant thickness of about 10% that of the gold layer, i.e. ~6 nm according to the FIB-SEM measurement for the gold thickness. The slightly deeper "Ag" peak shows that the Ag:S ratio is increasing with depth; the data suggests, but cannot prove (since the signal could also originate from a fragmentation of silver sulphide), that the silver could be metallic at the base of the sulphide layer. However, the following "AgAu" peak clearly demonstrates the presence of a thin intermixing layer at the top interface of the gold layer. The depth profile of "na_b" also exhibits narrow peaks of "Ag" and "AgAu" in the first few data points at the surface. Although within the transient regime, these peaks suggest that a very thin and sharp layer of silver has formed at the surface of gold

[5] The thickness of the intermixing layer can be estimated by the width of the AgAu peak at its half-maximum.

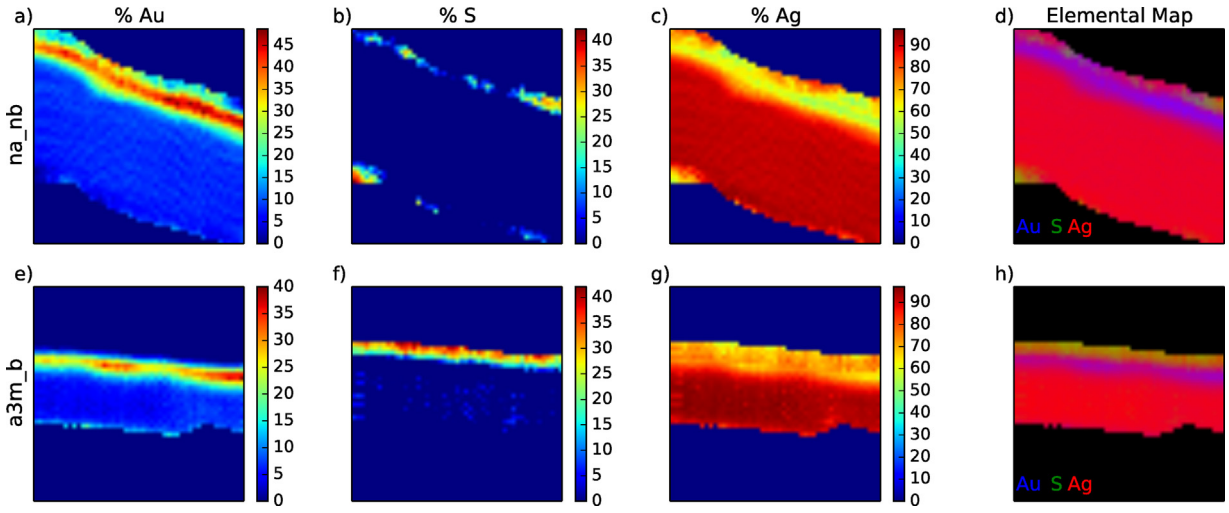

Fig. 6. STXM-derived elemental composition maps in terms of the percentage number of atoms, for a–d: "na_nb" and e–h: "a3m_b" Zwischgold sample cross-sections. Image size: 1 × 1 μm.

(≤ 2 nm) even on a non-aged sample.[6] However, no Ag corrosion is observed in this case.

5.3. Layer compositions

Examining the STXM elemental composition maps for the "na_nb" sample cross-section in Fig. 6a–d, we see two major layers, with a strong Au signal in the upper layer and a thicker layer of mostly Ag below. There is also some S detected at the upper and lower surfaces. The "gold" layer shows variations in the Au concentration, ranging between about 35% and 50%, but nowhere close to the 92% Au observed by RBS in the "na_nb" and "na_b" samples. The STXM Au map of "a3m_b" in Fig. 6e shows an even lower Au concentration, varying between about 25% and 40%. Both samples further show a 5%–10% Au concentration throughout the lower "silver" layer (Fig. 6a and e), in disagreement with the RBS observation of high purity silver in this layer. Interestingly, if we calculate the global composition from the "na_nb" STXM data, we get 13.6% Au, 84.8% Ag and 1.6% S, which is close to the 16.9% Au and 83.1% Ag calculated from RBS. This indicates that there has been a significant migration of both gold and silver in the STXM sample cross-sections. This effect will be discussed further in the following section with the example of an STEM lamella sample. According to *Noris Blattgold*, the Zwischgold foils were manufactured with 23.2 karat gold [45], equivalent to a purity of 96%. Therefore, the lower gold purity measured in the non-aged samples by RBS (92%) must be due to the interdiffusion of gold and silver.

5.4. Corrosion mechanism for unvarnished Zwischgold

Further examining the STXM composition maps for the "a3m_b" cross-section in Fig. 6f, g, a surface layer of about 30% S and 70% Ag can be seen, consistent with a Ag_2S corrosion layer. The composition of this corrosion layer shows a trend of decreasing S proportion with increasing depth, in agreement with the TOF-SIMS data.

SEM-EDX measurements of two aged samples (3-month and 35-year) showed that the dominant silver corrosion product was silver sulphide (S4.2 and S4.3 in Supplementary data), which deposits mainly on top of the gold layer and partially on the bottom of the silver layer (S3 in Supplementary data). The porous morphology of the silver sulphide surface layer is clearly observed in Fig. 7, demonstrating that it cannot form an effective barrier to air. When Au and Ag remain well adhered, no significant Ag corrosion products are observed at the Au/Ag interface. In the 35-year old sample, a significant delamination of the Zwischgold foil from the bole layer is observed (Fig. 7). This indicates that silver continues diffusing through the gold and transforming into silver corrosion products when there is no protection barrier, such as varnish, between the foil surface and air; eventually, the metallic silver will be fully depleted, causing complete delamination.

Besides the aged samples, a small amount of silver sulphide has also been detected on the top surface of non-aged Zwischgold samples through STXM (Fig. 6b–d), as we already discussed in Section 5.3. SEM-EDX spot tests support this observation (S3 in Supplementary data). This demonstrates that when no protective varnish applied, silver diffuses through gold and oxidizes on top of the gold layer at a relatively rapid speed, even at room temperature.

The 35-year old sample was further investigated by high-resolution STEM. The SE image for the ultra thin cross-section lamella (50 nm) shows a clear layering of porous silver sulphide, gold and silver, as well as a void between the foil and the bole (Fig. 8a), when the lamella was cut. However, after one night storage at room temperature in a vacuum desiccator, silver was observed to have migrated so rapidly that it already covered all other layers (Fig. 8b), which caused difficulty in the STEM measurements. In spite of this issue, STEM-EDX data on the area where the migrated silver layer was disturbed by irradiation of the electron beam (Fig. 8b, inside the red circle) still confirms that Ag exists mainly above and beneath the Au layer, and there is a gap inside of the original Ag layer (Fig. 9). S fluorescence is observed in a band coincident with the Au layer (although this is false[7]) and the upper Ag region, indicating that silver sulphide is mainly aggregated on the top surface of the Zwischgold foil. Note that there is a composition gradient in the silver sulphide layer, in agreement with the TOF-SIMS and STXM

[6] The first few data points are subject to possibly large intensity variations due to initial surface chemistry changes (transient regime), and the silver surface layer appears thinner than the depth resolution, so an accurate quantification is not possible.

[7] The S signal has some crosstalk from the Au signal, due to overlap of the XRF fluorescence peaks. Therefore, the region with Au appears to have S, but closer examination of the measured spectra shows this to be false (Section S5 in Supplementary data.

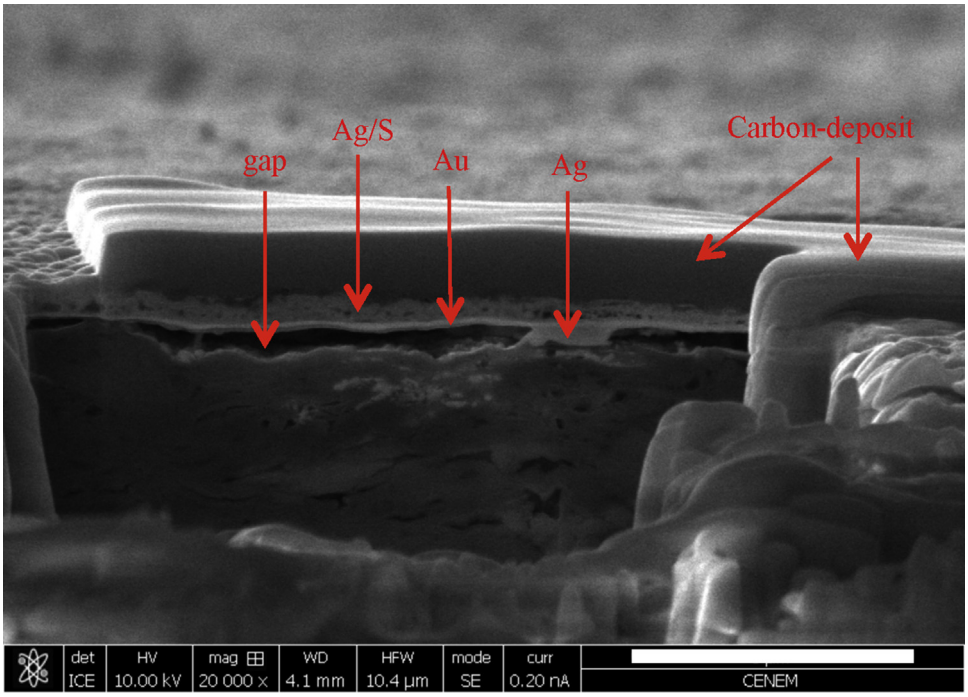

Fig. 7. SE micrograph through "FEI Helios Nanolab 660" for the 35-year old Zwischgold sample cross-section (Mag 20,000×). Scale bar: 3 µm.

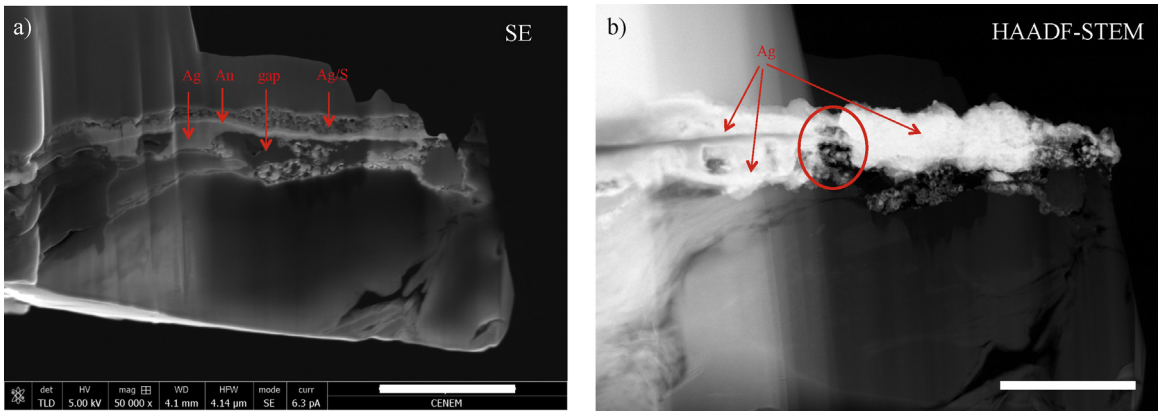

Fig. 8. a: SE micrograph through "FEI Helios Nanolab 660" for the cross-section lamella of the 35-year old Zwischgold sample (Mag 50,000×), taken when the lamella was cut; b: high-angle annular dark-field (HAADF) micrograph through "Titan Themis3 300" for the same lamella after one night storage at room temperature in vacuum; silver has migrated to cover all other layers. Scale bar: 1 µm.

observations. The chlorine fluorescence map displays only background noise.

The ageing and corrosion processes of unvarnished Zwischgold can be summarised as:

- at ambient temperature, silver atoms diffuse through the gold layer and accumulate on top of the gold surface, forming a thin silver layer;
- this thin, diffused silver surface layer interacts with oxidizing compounds in the atmosphere in the presence of water, producing corrosion products such as silver sulphide;
- since this corrosion layer does not function as an effective barrier against further corrosion, its thickness increases based on the consumption of metallic silver, as silver continues to diffuse through the gold layer;
- the migration of atoms away from the silver layer gradually increases the porosity and large voids within the silver until delamination eventually occurs between Zwischgold and its substrate.

A schematic illustration of the corrosion process of Zwischgold is presented in Fig. 10.

5.5. Implications for conservation

Regarding the conservation of historical artefacts with corroded Zwischgold surfaces, many restorers prefer to avoid any intervention, because removing the silver corrosion layer would accelerate the corrosion process. However, restorers need to be aware that the silver corrosion layer will only slow the corrosion process and cannot completely halt further corrosion. This is due to the porous morphology of silver sulphide [46] that is also observed in both normal (Fig. 7) and thin (Fig. 8a) cross-sections of our 35-year old sample. If no barrier is applied to protect the Zwischgold surface from air, then the Ag corrosion and diffusion will slowly

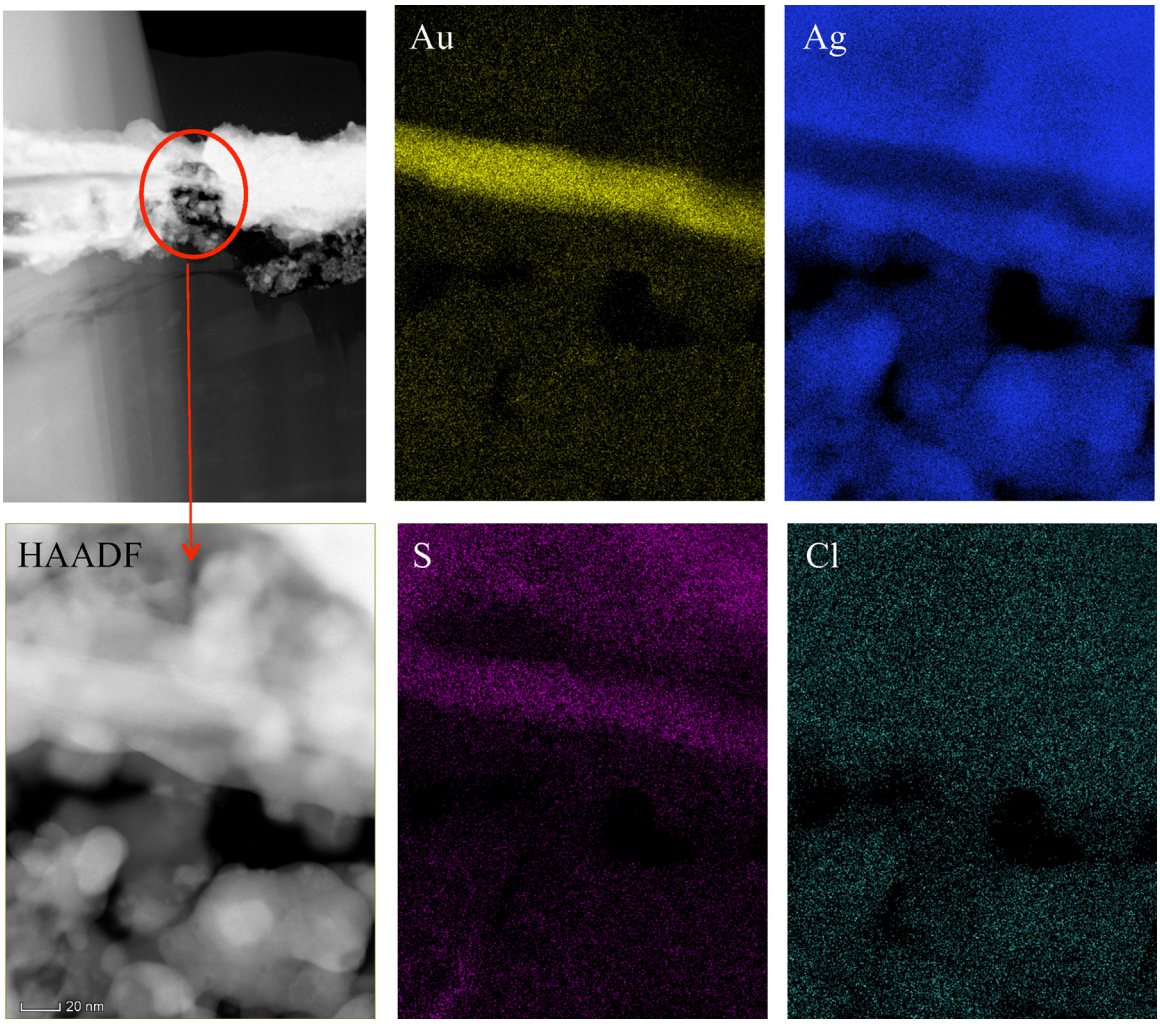

Fig. 9. STEM-EDX element mapping for the 35-year old sample. Note that the S signal has crosstalk from the Au signal and so some S falsely appears to be present in areas with a high Au concentration.

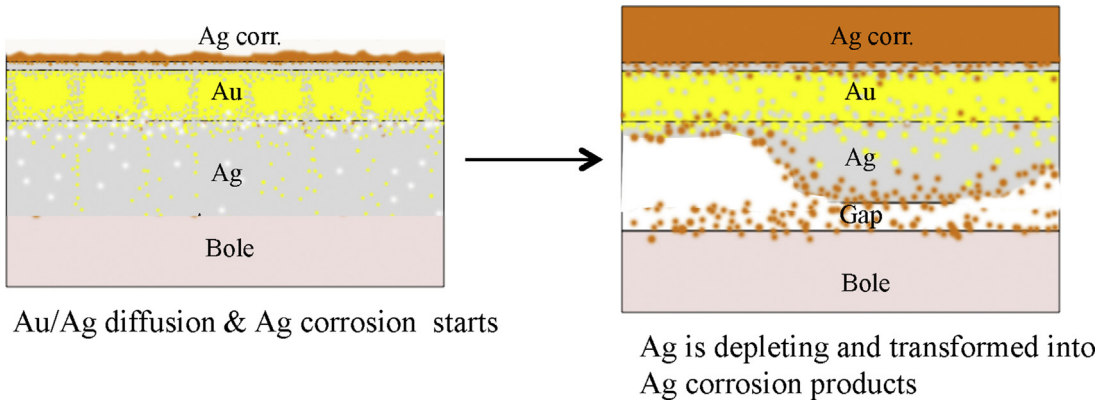

Fig. 10. Schematic illustration of the corrosion process of Zwischgold without varnish applied.

proceed until the base Ag layer is eventually exhausted, leaving a gap that reduces the stability of the foil on its substrate. In the long-term therefore, applying an extra barrier coating is recommended, which should be durable, provide sufficient protection as well as mechanical stabilization, and not disturb the original materials of the artefacts. Finding such a coating is an important research topic in the conservation of Zwischgold. However, any surface treatment of historical Zwischgold, such as the removal of degraded varnish, needs to be carried out with special care due to the delamination process taking place between the metal foil and its substrate.

The conservation and restoration of silver objects have been heavily discussed. Common conservation recommendations include avoiding high relative humidity, minimizing the concentration of invading species in the environment and also avoiding direct light illumination [41], which can be applied to the Zwischgold artefacts as well. Regarding invading species in the atmosphere,

it has been suggested that carbonyl sulphide (COS) might be more important than hydrogen sulphide (H_2S) in museum environments, since it was observed to have a higher and more stable concentration, regardless of geographic location [47]. Sources of COS include car exhaust, high temperature combustion and atmospheric photochemistry.

6. Conclusions

In this paper, the foil structure and aging mechanisms of unvarnished Zwischgold models/object have been presented. The overall foil thickness of modern Zwischgold varies in the range of 500–700 nm and the gold layer is equal to or less than 110 nm. The burnishing during the production of Zwischgold models does not inflict an obvious compress to the thickness of Zwischgold. There is no sharp gold and silver interface, even for non-aged Zwischgold samples. The gold layer inside Zwischgold is not pure, at least partially due to the gold and silver interdiffusion. The aesthetic difference between gold and Zwischgold can be also attributed to the diffusion of silver through the gold layer and accumulating on the top surface of Zwischgold. We have observed that this silver surface layer corrodes during exposure to air and this corrosion drives further silver diffusion until the base silver layer is exhausted, leaving a void between the foil and the bole. The silver sulphide corrosion products do not provide a complete barrier to further exposure to air and so the corrosion process will continue unless an extra barrier is provided, or the environment is appropriately controlled.

The high consistency of the experimental results demonstrate that the techniques applied in the project are suitable and efficient for the investigation of Zwischgold, which is important for the further study of historical Zwischgold samples. However, special attention needs to be given to the sample preparation and storage for experiments that require thin sample lamellas. FIB is recommended for the preparation of thin lamellas and normal cross-sections, due to the very high quality attainable. The latter can be also cut with ultra-microtome for a smooth face, which requires an embedding resin with similar hardness of the sample embedded. Our experience suggests it is necessary to keep silver-containing sample lamellas under cryogenic conditions to suppress the mobility of the silver atoms over the fresh-cut surfaces, as appears to have affected our STXM and STEM measurements.

As a first step in the study of Zwischgold, our investigation has been restricted to unvarnished Zwischgold models. However, in practice most of the historical Zwischgold artefacts have been protected with varnish during the production of the artworks, preventing oxidation. Some of them have even experienced more complicated situations such as being applied with multiple varnish layers at different times, under coloured glazing [48] or overpainted layers [26], or even with gold foils during restoration processes [49]. Therefore, the aging mechanisms of such artefacts could be diverse and complex. The study of historical samples will give more interesting information about materials, techniques and aging mechanisms of this special metal foil.

Acknowledgements

The authors thank Anna Bartl for helpful discussions and the access to the museum objects, and also thank Alexandra Roth for conventional TEM data, Meret Haudenschild, Klaus-Peter Urban, Kathrin Harsch, Martina Schönberg, Brigitte Lienert-Pärli and Blagoj Sarafimov for technical assistance. We thank Diamond Light Source for access to beamline I08 that contributed to the STXM results presented here (proposal SP15595). We also thank Dr. Eugenie Kirk for producing an Au/Ag alloy reference sample.

This work was supported by the Research Area "Materiality of Art and Culture" of the Bern University of the Applied Science – Bern University of the Arts (Switzerland), Paul Scherrer Institute (Switzerland) and Bernische Denkmalpflege – Stiftung (Switzerland). MM and RHF acknowledge financial support through GRK 1846 and BMBF, contract 05K16WED.

Appendix A. Supplementary data

Supplementary data associated with this article can be found, in the online version, at https://doi.org/10.1016/j.culher.2017.12.005.

References

[1] J.M. Nadolny, The techniques and use of gilded relief decoration by northern European painters, C. 1200–1500 (Doctor Thesis), Courtauld Institute of Art, London, 2000 (Chapter 8).
[2] S. Dietz, Malen mit Glas – Studien zur Maltechnik von Hans Holbein d. Ä (Dissertation), die Staatlichen Akademie der Bildenden Künste, Stuttgart, 2015, pp. 229–230.
[3] A. Burmester, U. Haller, C. Krekel. Pigmente et Colores: the Artist's Palette in Pharmacy Price Lists from Liegnitz (Silesia). In: Jo Kirby, Susan Nash und Joanna Cannon. Trade in Artists' Materials: Markets and Commerce in Europe to 1700. London, Archetype Publications Ltd. 2010, pp. 320.
[4] R. Eitelberger von Edelberg, Quellenschriften für Kunstgeschichte und Kunsttechnik des Mittelalters und der Renaissance. I. Cennino Cennini Das Buch von der Kunst, Osnabrück, Zelle, 1970, pp. 62.
[5] R.E. Straub, Tafel- und Tüchleinmalerei des Mittelalters. Reclams Handbuch der künstlerischen Techniken. Bd. 1, Philipp Reclam jun, Stuttgart, 1984, pp. 183–184.
[6] C. Zindel, Güldene Kunst-Pforte: Quellen zur Kunsttechnologie, in: Schriftenreihe Konservierung und Restaurierung der Hochschule der Künste Bern, Westermann Druck, Zwickau, 2010, pp. 679.
[7] E. Skaug, "Delt Gull" – "Laminatgull"? Problemer i medelalderens förgyllningstekkniker, in: Preprints nordisk Konservatorförbunds Kongress 9, 25–29 mai, 1981.
[8] H. Huth, Künstler und Werkstatt der Spätgotik, 3rd ed., Wissenschaftliche Buchgesellschaft, Darmstadt, 1977, pp. 97–98.
[9] E. Berger, Quellen und Technik der Fresko-, Oel- und Tempera-Malerei des Mittelalters von der byzantinischen Zeit bis einschließlich der 'Erfindung der Ölmalerei' durch die Brüder van Eyck, Neudr. Walluf/Nenedeln, München 1912, 1973, pp. 195.
[10] W.O. Akande, Y. Cao, N. Yao, N. Soboyejo, Adhesion and the cold welding of gold-silver thin films, J. Appl. Phys. 107 (043517) (2010), http://dx.doi.org/10.1063/1.3305791.
[11] P. Theophilus, E. Brephol, Theophilus Presbyter und das mittelalterliche Kunsthandwerk: Gesamtausgabe der Schrift "De diversis artibus". Bd. 2, Böhlau, Köln, 1999, pp. 127 (214).
[12] R. Kühnen, Der Ortenberger Altar aus dem Hessischen Landesmuseum Darmstadt: Untersuchungen und Anmerkungen zu technologischen Besonderheiten, Akademie der Bildenden Künste, Diplomarbeit, Stuttgart, 1997, pp. 31 (69–77).
[13] T. Brachert, Die Techniken der polychromierten Holzskulptur, Maltechnik Restauro 78 (1972) 189.
[14] F. Preusser. Die naturwissenschaftliche Untersuchung der Grünewaldtafeln aus Lindenhardt und ihre Ergebnisse. In: Die Lindenhardter Tafelbilder von Matthias Grünewald Bayerisches Landesamt für Denkmalpfleg, München 1978, pp. 20.
[15] P. Ta°ngeberg, Mittelalterliche Holzskulpturen und Altarschreine in Schweden: Studien zu Form, Material und Technik, Kungl. Vitterhets Historie och Antikvitets Akademien, Stockholm, 1986, pp. 223–227.
[16] J.M. Cröker, Der wohl anführende Mahler, Cröker, Jena, 1736, pp. 125 (cited from Kühnen 1997, pp. 75; Schiessl 1983, pp. 171).
[17] R.E. Straub, E.-L. Richter, H. Härlin, W. Brandt. Der Magdalenenaltar des Lucas Moser, eine technologische Studie. In: Beiträge zur Untersuchung und Konservierung mittelalterlicher Kunstwerke, Deutscher Kunstverlag München, 1974, pp. 41.
[18] K. Wittenburg, Der Traminer Altar im Bayerischen Nationalmuseum, München: Studien zu dem Hans Klocker zugeschriebenen Retabel (Diplomarbeit), Technische Universität München, München, 2004, pp. 32 (39, 47, 48, 53, 59, 84 & 108).
[19] K. von Baum, T. Neuhoff, C. von Saint-George, I. Schaefer, Blattmetallauflagen, Verzierungstechniken und Farbauftrag: Die künstlerische Handschrift aus technologischer Sicht, Zeitschrift für Kunsttechnologie und Konservierung (ZKK) 26 (2012) 33–53 (Heft 1).
[20] H. Huth, Künstler und Werkstatt der Spätgotik, 3rd ed., Wissenschaftliche Buchgesellschaft, Darmstadt, 1977, pp. 63.
[21] U. Schiessl, Techniken der Fassmalerei in Barock und Rokoko: dass Alles Von Bronce Gemacht Zu Sein Scheine, Worms, Werner, 1983, pp. 157.
[22] T. Brachert, F. Kobler, Fassung von Bildwerken, in: Reallexikon zur deutschen Kunstgeschichte. Bd. 7, Farbe, Farbmittel-Fensterladen, Verlag C.H. Beck, München, 1981 (Spalte 769).

[23] F. Buchenrieder, H. Kühn, T. Brachert, F. Kobler, Gefasste Bildwerke: Untersuchung und Beschreibung von Skulpturenfassungen mit Beispielen aus der praktischen Arbeit der Restaurierungswerktstätten des Bayerischen Landesamtes für Denkmalpflege 1958–1986, Lipp, München, 1990, pp. 73 (Vol. 40, Arbeitsheft – Bayerische Landesamt für Denkmalpflege. 74 & 81).
[24] J.S. Halle, Werkstätte der heutigen Künste. Bd. 15, Abteilung "Der Gold Schläger", Brandenburg und Leipzig, 1761, pp. 175 (cited from Kühnen 1997, pp. 75).
[25] T. Bullinger, Der Leiggerer Altar im Schweizerischen Landesmuseum: Eine kunstgeschichtliche und technologische Monographie (Dissertation), Albert-Ludwigs-Universität zu Freiburg i.Br., Urbach, 1974, pp. 225.
[26] M. Eveno, et al., The Louvre crucifix by Gioto: unveiling the original decoration by 2D-XRF, X-ray radiography, Emissiography and SEM-EDX analysis, Herit. Sci. 2 (2014) 17, http://dx.doi.org/10.1186/s40494-014-0017-y.
[27] M. Eveno, E. Martin, Les feuilles mixtes or-argent en peinture de chevalet. ICOM committee for Conservation. Painting II: Scientific study of paintings, James & James, London, 1996, pp. 355–359.
[28] C. Herm, Mobile micro-X-ray fluorescence analysis (XRF) on medieval paintings, Conserv. Cult. Herit. Chimia 62 (11) (2008) 887–898, http://dx.doi.org/10.2533/chimia.2008.887.
[29] A. Mounier, F. Daniel, Sgraffito, zwischgold et brocart applique la dorure dans tous ses états au sein de quelques peintures murales (XI–XVI siècle) due Sud-Ouest de la France, ArcheoScience Rev. Archeometr. 37 (2013) 33–40.
[30] C. Serendan, D. Hradil, J. Hradilová, J. Cannataci, Early Renaissance altarpieces in Transylvania: materials and technological characteristics, in: Renaissance Workshop: The Materials and Techniques of Renaissance Art, Archetype Publications, London, 2013, pp. 60–70.
[31] B. Hartwieg, Kunsttechnologische Analyse des Göttinger Barfüßerretabels von 1424 im Kontext zeitgenössischer norddeutscher Altarwerke (Dissertation), Hochschule für Bildende Künste Dresden, Dresden, 2010, pp. 128–129 (199–200).
[32] U. Plahter, Norwegian art technology in the twelfth and thirteenth centuries: materials and techniques in a European context, Zeitschrift für Kunsttechnologie und Konservierung (ZKK) 28 (2014) 298–333 (Heft 2).
[33] Personal communication with PD Dr. Heike Stege from Doerner Institute, Munich (22 June 2017).
[34] J.C.M. Hwang, J.D. Pan, R.W. Balluffi, Measurement of grain-boundary at low temperature by the surface-accumulation method. I. Method and analysis. II. Results for gold–silver system, J. Appl. Phys. 50 (1349) (1979), http://dx.doi.org/10.1063/1.326115.
[35] F.H. Buttner, E.R. Funk, H. Udin, Adsorption of oxygen on silver, J. Phys. Chem. 56 (1961) 657–660, http://dx.doi.org/10.1021/j150497a022.
[36] F.E. Bartel, J.T. Smith, Alteration of surface properties of gold and silver as indicated by contact angle measurements, J. Phys. Chem. 57 (2) (1953) 165–172, http://dx.doi.org/10.1021/j150503a008.
[37] Y.Y. Liu, L. Wang, J.Z. Zhan, L. Chui, An investigation of silver diffusion through gold films by Auger electron spectroscopy, Vacuum 35 (12) (1985) 537–538.
[38] T.E. Graedel, Corrosion mechanisms for silver exposed to the atmosphere, J. Electrochem. Soc. 139 (7) (1992) 1963–1970.
[39] H. Águas, et al., Study of environmental degradation of silver surface, Phys. Stat. Sol. (c) 5 (5) (2008) 1215–1218, http://dx.doi.org/10.1002/pssc.200777842.
[40] J.P. Franey, G.W. Kammlott, T.E. Graedel, The corrosion of silver by atmospheric sulfurous gases, Corrosion Sci. 25 (2) (1985) 133–143.
[41] M. Inaba, Tarnishing of Silver: A Short Review. Conservation Journal Jan. 1996 Issue 18, Victoria and Albert Museum, London, 1996 (Online: http://www.vam.ac.uk/content/journals/conservation-journal/issue-18/tarnishing-of-silver-a-short-review/).
[42] A. Bartl, C. Krekel, M. Lautenschlagger, D. Oltrogge, Der "Liber illuministarum" aus Kloster Tegernsee: Edition, Übersetzung und Kommentar der kunsttechnologischen Rezepte. Vol. Bd. 8, Steiner, Stuttgart, 2005 (Chapters 5 & 6).
[43] Personal communication with Prof. Volker Schaible from Staatliche Akademie der bildenden Künste Stuttgart (19 January 2017).
[44] M. Lerotic, R. Mak, S. Wirick, F. Meirer, C. Jacobsen, MANTiS (2014): a program for the analysis of X-ray spectromicroscopy data, J. Synchrotron Rad. 21 (5) (2014) 1206–1212, http://dx.doi.org/10.1107/S1600577514013964.
[45] M. Haudenschild, Zwischgold an mittelalterlichen Skulpturen, Altären und Reliefs: Überlegungen zum Vorkommen und der ursprünglichen Wirkung, 2016, pp. 9 (Bachelorthesis in Konservierung), Hochschule der Künste, Bern. fn. 14.
[46] P.G. Slade, Electrical Contacts: Principles and Applications, 2nd ed., CRC Press, Boca Raton, 2014 (Chapter 2).
[47] H.A. Ankersmit, N.H. Tennent, S.E. Watts, Hydrogen sulfide and carbonyl sulfide in the museum environment – Part I, Atmos. Environ. 39 (2005) 695–707, http://dx.doi.org/10.1016/j.atmosenv.2004.10.013.
[48] M. Eveno, E. Martin, C. Ressort, L'ornementation métallique et ses altérations, Techne 7 (1998) 105–108.
[49] G. Kerscher, "Geistliches Goldt" Bemerkungen zur Wiederherstellung der Erstfassung von St. Lorenz in Kempten, Zeitschrift für Kunsttechnologie und Konservierung (ZKK) 6 (1) (1992) 174–189.